

# Study on Transfer Function of Intra-Body Communication Based on Quasi-static Electric Field Modeling

X. M. Chen, S. H. Pun, Y. M. Gao, P. U. Mak, M. I. Vai and M. Du

**Abstract**—Transfer function analysis plays an important role in the investigation of intra-body communication (IBC). In this paper, the voltage distribution based on the quasi-static electric field modeling of human limb for galvanic coupling IBC is analyzed, transfer function of physical channel from 1 Hz to 1MHz is derived and proposed. The attenuation in transfer function shows that lower attenuation is obtained in frequency band from 20 kHz to 1 MHz. Moreover, rectangular pulse is utilized as the input to evaluate this system transfer function. The results in rectangular pulse response indicate separation of distance between transmitter and receiver is the major consideration in designing galvanic coupling IBC system. Finally, this paper reveals bit error rate (BER) under different distances for binary phase-shift keying (BPSK), quadrature phase-shift keying (QPSK) and 8PSK modulation schemes.

## I. INTRODUCTION

Body Area Network (BAN) is developed to facilitate low power devices operating on, in or around the human body to serve a variety of applications including medical and consumer electronics. The medical and health monitoring has caught the attention of the research groups. Building the health monitor BAN, extremely low power and high security radio is needed. The potential candidates include Zigbee, Bluetooth and Ultra Wide Band (UWB) and IBC[1, 2]. Compared with other transmission techniques, IBC consumes low power (<1mW), offers data rate fast enough for biotelemetry with high security by using the human body as the transmission medium[1, 2]. In IBC, the transmitted signal can be controlled by the electric current or the electric potential through the body, which we call galvanic coupling and capacitive coupling, respectively. Existing communication prototypes for the two coupling methods have reach data rate from several kbps to Mbps. Data rate of 2.4 kbps were achieved by Zimmerman[3]in the first successful personal area network by using a carrier of 330 kHz and OOK modulation scheme. A higher data rate of 9.6 kbps was obtained by utilizing the 10.7 MHz FSK transmitter

and receiver[4]. Kurt Partridge et al. in [5] extended the system of Zimmerman and built one with data rate up to 38.4 kbps using FSK. Japanese Nippon Telegraph and Telephone Corporation (NTT) and its subsidiary successfully realized communication in electronic device called RedTacton[6] with data rate up to 10 Mbps. However, the data rate reached depends on the working environment. Lin et al. in [7] developed the SOC system using the capacitive coupling IBC with a data rate of 2 Mbps. Wegmuller in [8, 9] investigated the signal attenuation in galvanic coupling IBC from 10 kHz to 1 MHz. The data rate of 64 kbps was achieved for a carrier frequency of 256 kHz in QPSK modulation.

The above IBC systems give us the data rate in data communication. However, the optimal modulation, data rate and concerning parameters in designing IBC system have not been fully addressed yet. The output in response to an input signal in the IBC system depends on the system transfer function[10]. To give some insight about consideration in designing IBC system, the paper will analyze the transfer function and the output in response to a rectangular pulse input. Data rates in modulation schemes of BPSK, QPSK and 8PSK will be investigated. Since in medical and healthcare application, the data rate can be low but the reliability is important requirement[2]. In galvanic coupling, all the current forming the closed loop circuit in the human body makes the communication system can tolerate and immune to the interference. Thus, the paper will analyze the physical channel of the galvanic coupling IBC based on the quasi-static electric field model.

Section 2 analyzes the quasi-static electric model of galvanic coupling IBC, obtains the transfer function up to 1MHz. Section 3 develops the rectangular pulse response of the IBC system, presents the critical parameters in designing data communication system and reveals the performance of different modulation schemes. Finally, section 4 concludes the paper.

## II. TRANSFER FUNCTION

There already have theoretical work related to quasi-static electric field modeling to study the mechanism of signal propagation in galvanic coupling IBC. In [11], Gao addressed the conductivity of the tissues and developed the quasi-static electric field model of galvanic coupling IBC. In [12], Pun and Gao extended the model considering both the conductivity and permittivity of human tissue. The calculation results in the above model have been proved by the experiment data not only limited to the surface of phantom, but also inside of various tissues. In this section, we

Manuscript received October 7th, 2011. This work was supported by The Science and Technology Development Fund of Macau under grant 014/2007/A1, 063/2009/A and 024/2009/A1, the Research Committee of University of Macau under Grants UL012/09-Y1/EEE/VMI01/FST, RG077/09-10S/VMI/FST, RG075/07-08S/10T/VMI/FST, and RG072/09-10S/MPU/FST.

X. M. Chen, S. H. Pun, P. U. Mak, and M. I. Vai are with the Electrical and Computer Engineering, Faculty of Science and Technology, University of Macau, Av. Padre Tomas Pereira, Taipa, Macau. (Tel: 853-83974276; fax: 853-83974275; e-mail: sammy.cxm@gmail.com).

Y. M. Gao and M. Du are with the Key Laboratory of Medical Instrumentation & Pharmaceutical Technology, Fujian Province, China and Institute of Precision Instrument, Fuzhou University, China.

continue to investigate the transfer function of IBC channel based on the quasi-static electric field model.

Considering the galvanic coupling IBC on the forearm, the human limb can be assumed to be a concentric cylinder representing by the skin, fat, muscle and bone layers with radius  $(r_1, \dots, r_4)$  from the center. As is depicted in Fig. 1, the medium is characterized by permittivity  $(\epsilon_1, \dots, \epsilon_4)$  and conductivity  $(\sigma_1, \dots, \sigma_4)$ .

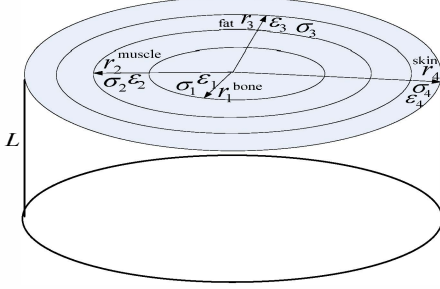


Fig. 1. Geometry of the human limb

The electrical characteristic of wet skin, fat, muscle and bone are concluded by Gabriel[13]. It is found in [11] that, at the frequency lower than 1MHz, The criteria of neglecting inductive effect and propagation effect is satisfied, while criteria of neglecting capacitance effect is not satisfied.

$$\text{Neglecting inductive effects} \quad (kR_{\max})^2 \ll 1 \quad (1)$$

$$\text{Neglecting capacitance effects} \quad \frac{\omega\epsilon}{\sigma} \ll 1 \quad (2)$$

$$\text{Neglecting propagation effects} \quad kR_{\max} \ll 1 \quad (3)$$

$$k^2 = \omega^2 \mu \epsilon (1 + \sigma / j\omega\epsilon) \quad (4)$$

Where  $\sigma$  is the conductivity,  $\epsilon$  is the permittivity,  $\omega$  is the frequency. In IBC, the absence of inductive material in human body so that the permeability  $\mu$  is that of the free space, and the transmission range in IBC specifies the overall dimension of human body as  $R_{\max} = 1$  for simplicity[14]. Applying the quasi-static approximation in [15] and Maxwell's equations[16], the governing function for potential in cylindrical coordinate system satisfied:

$$\nabla \cdot \sigma_{c(s)} \nabla V = \frac{1}{r} \frac{\partial}{\partial r} \left( r \frac{\partial V}{\partial r} \right) + \frac{1}{r^2} \frac{\partial^2 V}{\partial \phi^2} + \frac{\partial^2 V}{\partial z^2} = 0 \quad s = 1 \dots 4 \quad (5)$$

Where  $\sigma_{c(s)}$  is composite conductivity of layer  $s$ , and

$$\sigma_{c(s)} = \sigma_s + j\omega\epsilon_{rs}\epsilon_0 \quad (6)$$

Where  $\sigma_s$  and  $\epsilon_{rs}$  are the conductivity and relative permittivity of layer  $s$  respectively. And  $\epsilon_0$  is the permittivity of free space. The continuity of voltage in the tissue interface satisfies:

$$V_s(\phi, z) = V_{s+1}(\phi, z) \quad (7)$$

The normal component of electric field at the interface between two media must be continuous. That is:

$$\sigma_{c(s)} E_{sn} = \sigma_{c(s+1)} E_{(s+1)n} \quad (8)$$

Where  $\sigma_{c(s)}$  and  $\sigma_{c(s+1)}$  are the composite conductivity of

layer  $s$  and  $s+1$  respectively,  $E_{sn}$  and  $E_{(s+1)n}$  are the respective normal component of electric fields. The transverse section at the wrist is set to  $z = 0$ , and at the joint  $z = L$ . We have:

$$\begin{aligned} V(r, \phi, 0) &= 0 \\ V(r, \phi, L) &= 0 \end{aligned} \quad (9)$$

The current source is placed on the surface of human limb.

$$\frac{\partial V}{\partial r}(r = r_4, \phi, z) = -\nabla V = \frac{J_n(\phi, z)}{\sigma_4} \quad (10)$$

$$J_n(\phi, z) = \begin{cases} 1 & z_e \leq z < z_e + d \text{ and } 0 \leq \phi < 2\pi \\ -1 & z_e \leq z < z_e + d \text{ and } 0 \leq \phi < 2\pi \end{cases} \quad (11)$$

Where  $J_n$  is the normal component of current density,  $z_e$  and  $d$  are the position and height of the electrodes, respectively. The voltage distribution on the surface of the human limb will be:

$$\begin{aligned} V_4(r, \phi, z) &= \sum_{k=1}^{\infty} \sum_{n=1}^{\infty} [E_{4kn} I_n \left( \frac{k\pi}{L} r \right) \cos(n\phi) + F_{4kn} I_n \left( \frac{k\pi}{L} r \right) \sin(n\phi)] + \\ &G_{4kn} K_n \left( \frac{k\pi}{L} r \right) \cos(n\phi) + H_{4kn} K_n \left( \frac{k\pi}{L} r \right) \sin(n\phi) \sin \left( \frac{k\pi}{L} z \right) \end{aligned} \quad (12)$$

Where  $I_n$  is the modified Bessel function of the first kind of order  $n$ ,  $K_n$  is the modified Bessel function of second kind of order  $n$ ,  $E_{4kn}$ ,  $F_{4kn}$ ,  $H_{4kn}$  and  $G_{4kn}$  are the parameters on layer  $s = 4$  and can be solved by the (13), (14), (15) and (16).

$$E_{4kn} = \frac{P_{4kn} G_{4kn}}{Q_{4kn}} \quad (13)$$

$$F_{4kn} = \frac{M_{4kn} H_{4kn}}{O_{4kn}} \quad (14)$$

$$G_{4kn} = \frac{\alpha_4 Q_{4kn}}{\sigma_{c(s=4)} \left[ P_{4kn} I_n' \left( \frac{k\pi}{L} r_4 \right) + Q_{4kn} K_n' \left( \frac{k\pi}{L} r_4 \right) \right]} \quad (15)$$

$$H_{4kn} = \frac{\beta_4 O_{4kn}}{\sigma_{c(s=4)} \left[ M_{4kn} I_n' \left( \frac{k\pi}{L} r_4 \right) + O_{4kn} K_n' \left( \frac{k\pi}{L} r_4 \right) \right]} \quad (16)$$

And

$$\alpha_4 = \begin{cases} \frac{2}{\pi L} \int_0^L \int_0^{2\pi} J(\phi, z) \cos(n\phi) \sin \left( \frac{k\pi}{L} z \right) d\phi dz & n = 1, 2, \dots \\ \frac{1}{L} \int_0^L J(\phi, z) \sin \left( \frac{k\pi}{L} z \right) dz & n = 0 \end{cases} \quad (17)$$

$$\beta_4 = \begin{cases} \frac{2}{L\pi} \int_0^L \int_0^{2\pi} J(\phi, z) \sin(n\phi) \sin \left( \frac{k\pi}{L} z \right) d\phi dz & n = 1, 2, \dots \\ 0 & n = 0 \end{cases} \quad (18)$$

$$P_{skn} = \sigma_{c(s)} K_n' \left( \frac{k\pi}{L} r_{s-1} \right) \left[ P_{(s-1)kn} I_n \left( \frac{k\pi}{L} r_{s-1} \right) + Q_{(s-1)kn} K_n \left( \frac{k\pi}{L} r_{s-1} \right) \right] \quad (19)$$

$$- \sigma_{c(s-1)} K_n \left( \frac{k\pi}{L} r_{s-1} \right) \left[ P_{(s-1)kn} I_n' \left( \frac{k\pi}{L} r_{s-1} \right) + Q_{(s-1)kn} K_n' \left( \frac{k\pi}{L} r_{s-1} \right) \right]$$

$$Q_{skn} = \sigma_{c(s-1)} I_n \left( \frac{k\pi}{L} r_{s-1} \right) \left[ P_{(s-1)kn} I_n' \left( \frac{k\pi}{L} r_{s-1} \right) + Q_{(s-1)kn} K_n' \left( \frac{k\pi}{L} r_{s-1} \right) \right] \quad (20)$$

$$- \sigma_{c(s)} I_n' \left( \frac{k\pi}{L} r_{s-1} \right) \left[ P_{(s-1)kn} I_n \left( \frac{k\pi}{L} r_{s-1} \right) + Q_{(s-1)kn} K_n \left( \frac{k\pi}{L} r_{s-1} \right) \right]$$

$$M_{skn} = \sigma_{c(s)} K_n' \left( \frac{k\pi}{L} r_{s-1} \right) \left[ M_{(s-1)kn} I_n \left( \frac{k\pi}{L} r_{s-1} \right) + O_{(s-1)kn} K_n \left( \frac{k\pi}{L} r_{s-1} \right) \right] \quad (21)$$

$$- \sigma_{c(s-1)} K_n \left( \frac{k\pi}{L} r_{s-1} \right) \left[ M_{(s-1)kn} I_n' \left( \frac{k\pi}{L} r_{s-1} \right) + O_{(s-1)kn} K_n' \left( \frac{k\pi}{L} r_{s-1} \right) \right]$$

$$O_{skn} = \sigma_{c(s-1)} I_n \left( \frac{k\pi}{L} r_{s-1} \right) \left[ M_{(s-1)kn} I_n' \left( \frac{k\pi}{L} r_{s-1} \right) + O_{(s-1)kn} K_n' \left( \frac{k\pi}{L} r_{s-1} \right) \right] - \sigma_{c(s)} I_n' \left( \frac{k\pi}{L} r_{s-1} \right) \left[ M_{(s-1)kn} I_n \left( \frac{k\pi}{L} r_{s-1} \right) + O_{(s-1)kn} K_n \left( \frac{k\pi}{L} r_{s-1} \right) \right] \quad (22)$$

$$P_{1kn} = M_{1kn} = 1 \quad (23)$$

$$Q_{1kn} = O_{1kn} = 0 \quad (24)$$

Where  $[\ast]'$  indicates the first derivative of the argument. The transfer function of the body channel is (25):

$$H(f) = \frac{V_4(r, \phi, z2)}{V_4(r, \phi, z1)} \quad f < 1\text{MHz} \quad (25)$$

$$V_4(r, \phi, z1) = \sum_{k=1}^{\infty} \sum_{n=1}^{\infty} [E_{4kn} I_n \left( \frac{k\pi}{L} r \right) \cos(n\phi) + F_{4kn} I_n \left( \frac{k\pi}{L} r \right) \sin(n\phi) + G_{4kn} K_n \left( \frac{k\pi}{L} r \right) \cos(n\phi) + H_{4kn} K_n \left( \frac{k\pi}{L} r \right) \sin(n\phi)] \cdot \sin \left( \frac{k\pi}{L} z1 \right) \quad (26)$$

$$V_4(r, \phi, z2) = \sum_{k=1}^{\infty} \sum_{n=1}^{\infty} [E_{4kn} I_n \left( \frac{k\pi}{L} r \right) \cos(n\phi) + F_{4kn} I_n \left( \frac{k\pi}{L} r \right) \sin(n\phi) + G_{4kn} K_n \left( \frac{k\pi}{L} r \right) \cos(n\phi) + H_{4kn} K_n \left( \frac{k\pi}{L} r \right) \sin(n\phi)] \cdot \sin \left( \frac{k\pi}{L} z2 \right) \quad (27)$$

Where  $V_4(r, \phi, z1)$  and  $V_4(r, \phi, z2)$  is the voltage at the position of  $(r, \phi, z1)$  and  $(r, \phi, z2)$  in cylindrical human limb, respectively. According to the transfer function, the attenuation is:

$$\text{Attention}(f) = 20 \cdot \log_{10}(H(f)) \quad f < 1\text{MHz} \quad (28)$$

### III. SIMULATION AND RESULTS

#### A. Attenuation and Frequency

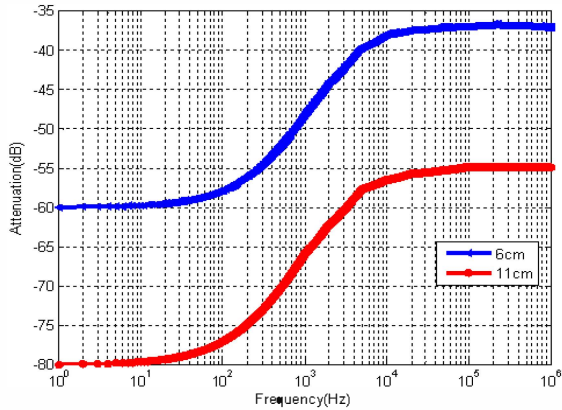


Fig. 2. Attenuation in distance separation of 6cm and 11cm

Assume the length of human limb is 30 centimeter (cm), the dimension of the electrode is 4cm by 4cm, the injected current is 1 milliampere (mA). As the transfer function in (25), the attenuation for the operating frequency between 1 Hz and 1 MHz in a distance of 6cm and 11cm separation between transmitter and receiver are showed in Fig. 2. The attenuation is about -60dB and -80dB for operating frequency below 10 Hz at a distance of 6cm and 11cm, respectively. And the attenuation decreases gradually as the frequency increases, sustains almost -37dB and -55dB for the frequency higher than 20 kHz in 6cm and 11cm, respectively. Attenuation in system transfer function indicates that low frequency components of spectrum of the signal transmitted through the

channel will suffer higher attenuation compared to high frequency components. Thus, the transmitted signal should be modulated to the frequency that is higher than 20 kHz and lower than 1 MHz.

#### B. Consideration in Designing IBC System

The most basic information unit in a digital transmission scheme is a rectangular pulse[17]. Thus, we send a rectangular pulse at the transmitter and analyze the distortion caused by the IBC channel at the receiver. The output should be the Inverse Fourier Transform (IFT) of the product of the input Fourier Transform (FT) and the transfer function. The spectrum of the rectangular pulse is the *Sinc* function[10]. The range of energy concentration in *Sinc* function is the null to null bandwidth. And the bandwidth is inverse proportion to the pulse width. For sake of comparison, we consider pulse width of 1 millisecond (ms) and 0.1ms. The two rectangular pulses will be transmitted through the channel represented by (25) with the carrier of 500 kHz. The input and received signals with a distance of 6cm and 11cm are showed in Fig. 3.

From the result presented in Fig. 3, the outputs are the rectangular pulses. According to calculation result, the rise time of the outputs is smaller than 1% of the pulse width. With different pulse width, both the outputs at a distance of 6cm are almost the same, so are the outputs at 11cm. The amplitude of outputs at 11cm is much lower than that at 6cm. Distance between transmitter and receiver have great effects in the output. Thus, as the bandwidth of the signal is smaller than that of IBC channel, and the signal is modulated to high frequency around 500 kHz, distance separation of transmitter and receiver is a major concern in frequency channel between 1 Hz and 1MHz in designing IBC system.

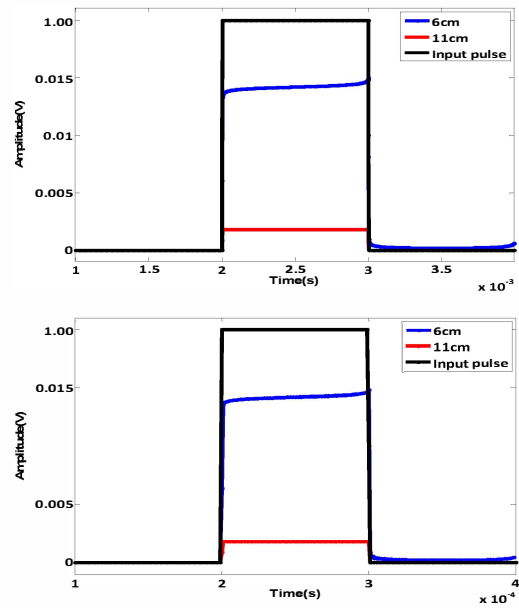


Fig. 3. Output of rectangular pulse (pulse width: 1ms & 0.1ms) with carrier 500 kHz

### C. Performance of Modulation Schemes

In order to evaluate the effect on performance in data communication caused by distance, and obtain the most suitable modulation scheme with low BER, we study the data rate and BER performance of the modulation scheme BPSK, QPSK and 8PSK. The symbol burst will be shaped by the square root raised cosine filter with  $\alpha=0.5$  to minimize the Inter Symbol Interference (ISI). The attenuated signal will be distorted by the Additive White Gaussian Noise (AWGN) in the channel. We assume the noise power spectral density (PSD) is  $1e^{-7} \text{ V}/\sqrt{\text{Hz}}$ , which is 100 times higher than that in [10]. The BER is calculated as a function of bit rate under different distances for each modulation scheme. We found that at the distance of 6cm, all the modulation schemes have the BER lower than  $1e^{-4}$  under the bit rate of 200 kbps. In Fig. 4, the BER performance of BPSK, QPSK and 8PSK are showed for data rates between 10 kbps and 100 kbps for a distance of 11 cm.

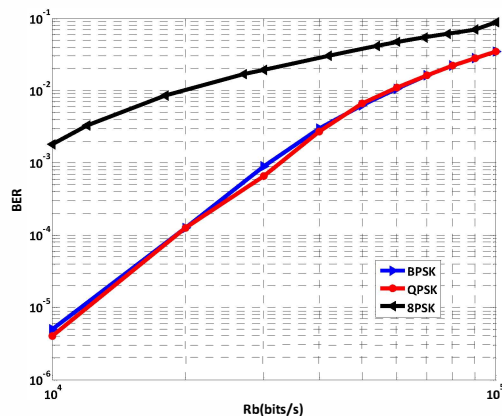


Fig. 4. Performance of different modulation schemes

As is depicted in Fig. 4, the performance of BPSK and QPSK is almost the same, with that of QPSK is better than BPSK slightly. The result is comparable to the result obtain by Marc Wegmueller et al.[18]. The BER is lower than  $1e^{-3}$  at the maximum bit rate of 30 kbps in BPSK and QPSK modulation. The BER is lower than  $1e^{-2}$  as the bit rate lower than 20 kbps in 8PSK. Considering the bandwidth efficiency, 8PSK has the highest bandwidth efficiency. However, the 8PSK can not tolerate the high noise, and suffers high BER. In a word, 8PSK trades bandwidth efficiency off BER. While the bandwidth efficiency of QPSK is twice as high as that of BPSK, and QPSK obtains lowest BER. Thus, consideration the bandwidth efficiency and BER, QPSK modulation scheme has the highest bit rate with low BER and is the optimal modulation scheme among BPSK, QPSK and 8PSK in the short distance.

### IV. CONCLUSION

We have analyzed the quasi-static electric field model of galvanic coupling IBC. The attenuation in transfer function shows higher gain is obtained in the high frequency. The

result revealed that large bandwidth up to several hundred kHz obtains low distortion in the frequency band between 20 kHz and 1 MHz. By analyzing output of pulse with different bandwidth, we found out that distance between transmitter electrodes and receiver is a critical parameter in designing the IBC communication system, which is a helpful result for the IBC system design. Finally, QPSK modulation scheme obtained the best performance among BPSK, QPSK and 8PSK modulation schemes in short distance with noise environment with PSD up to  $1e^{-7} \text{ V}/\sqrt{\text{Hz}}$ .

### REFERENCE

- [1] V. Lucev, I. Krois, and M. Cifrek. Intrabody communication in biotelemetry. *Wearable and Autonomous Biomedical Devices and Systems for Smart Environment*, 2010, vol. 75, pp. 351-368. Available: <http://www.springerlink.com/content/vgn2v153376372226/>
- [2] H.B. Li and R. Kohno. Body area network and its standardization at IEEE 802.15. BAN. *Advances in Mobile and Wireless Communications*, 2008, vol. 16, pp. 223-238. Available: <http://www.springerlink.com/content/h3715768w871590j/>
- [3] T.G. Zimmerman, "Personal area networks: near-field intrabody communication." PhD thesis, Massachusetts Institute of Technology, 1995.
- [4] K. Hachisuka, A. Nakata, T. Takeda, et al., "Development and performance analysis of an intra-body communication device." *Proc. of 12<sup>th</sup> International Conference on Solid State Sensors, Actuators and Microsystems*, pp. 1722-1725, 2003.
- [5] K. Partridge, B. Dahquist, et al. "Empirical measurements of intrabody communication performance under varied physical configurations." in *Proc. 14th ACM . User Interface Software and Technology*, 2001, pp. 183-190.
- [6] NTT, Advanced communication through flesh Redtacton. Available: <http://www.technicalsymposium.com/abstract9.doc>
- [7] Y.T. Lin, Y.S. Lin and S.S. Lu, "A 0.5-V biomedical System-on-a-Chip for intrabody communication system." *IEEE Transactions on Industrial Electronics*, 2011, 58(2): pp. 690-699.
- [8] M.S. Wegmueller, A. Kuhn, et al., "An attempt to model the human body as a communication channel." *IEEE Transactions on Biomedical Engineering*, 2007, 54(10): p. 1851-1857.
- [9] M.S. Wegmueller, "Intra-body communication for biomedical sensor networks." PhD. dissertation, ETH Zurich, 2007.
- [10] J. Chitode, *Continuous Time Signal And Systems*. 2006: Technical Publications, pp:1-5, 210-216.
- [11] Y.M. Gao, S.H. Pun, et al., "Quasi-static field modeling and validation for intra-Body communication." *The 3rd Int. Conf. Bioinformatics and Biomedical Engineering*, Beijing, 2009, pp. 1-4.
- [12] S.H. Pun, Y.M. Gao, et al., "Quasi-static modeling of human limb for intra-body communications with experiments." *IEEE Trans. Inf. Technol. Biomed.*, 2011.
- [13] C. Gabriel, "Compilation of the dielectric properties of body tissues at RF and microwave frequencies." *Med. Biol.*, vol. 41, pp.2231 - 2249 , 1996.
- [14] R. Plonsey and D.B. Heppner, "Considerations of quasi-stationarity in electrophysiological systems." *Bulletin of Mathematical Biology*, 1967, 29(4): p. 657-664.
- [15] J. Larsson, "Electromagnetics from a quasistatic perspective." *American Journal of Physics*, 2007, 75: p. 230.
- [16] B.S. Guru and H.R. Hrozlu, *Electromagnetic field theory fundamentals*. 2004: Cambridge University Press, pp: 286-309.
- [17] K. Gentile, "Digital pulse-shaping filter basics." Analog Devices, AN-922 Application Note. Available: [http://www.newark.thinkhost.com/brands/promos/leading\\_edge/AN-922\\_AD7765.pdf](http://www.newark.thinkhost.com/brands/promos/leading_edge/AN-922_AD7765.pdf)
- [18] M.S. Wegmueller, W. Fichtner, et al."BPSK & QPSK modulation for biomedical monitoring sensor network." in *Proc. 28th IEEE EMBS Annu. Inter. Conf.*, New York, 2006.